Applied Physics Letters

An *in situ* x-ray photoelectron spectroscopy study of the initial stages of rf magnetron sputter deposition of indium tin oxide on p-type Si substrate

Cite as: Appl. Phys. Lett. **102**, 021606 (2013); https://doi.org/10.1063/1.4774404
Submitted: 27 October 2012 • Accepted: 20 December 2012 • Published Online: 17 January 2013

M. H. Rein, M. V. Hohmann, A. Thøgersen, et al.

View Online

Export Citation

CrossMark

ARTICLES YOU MAY BE INTERESTED IN

Elemental distribution and oxygen deficiency of magnetron sputtered indium tin oxide films
Journal of Applied Physics **109**, 113532 (2011); https://doi.org/10.1063/1.3587174

Initial stages of ITO/Si interface formation: In situ x-ray photoelectron spectroscopy measurements upon magnetron sputtering and atomistic modelling using density functional theory
Journal of Applied Physics **115**, 083705 (2014); https://doi.org/10.1063/1.4866991

Electrical, optical, and structural properties of indium-tin-oxide thin films for organic light-emitting devices
Journal of Applied Physics **86**, 6451 (1999); https://doi.org/10.1063/1.371708

Webinar
Quantum Material Characterization for Streamlined Qubit Development

Zurich Instruments

Register now

AIP Publishing

© 2013 American Institute of Physics.

An *in situ* x-ray photoelectron spectroscopy study of the initial stages of rf magnetron sputter deposition of indium tin oxide on p-type Si substrate

M. H. Rein,[1,a] M. V. Hohmann,[2] A. Thøgersen,[3] J. Mayandi,[4] A. O. Holt,[1] A. Klein,[2] and E. V. Monakhov[1,5]

[1]*Institute for Energy Technology, Department of Solar Energy, Instituttveien 18, 2008 Kjeller, Norway*
[2]*Technische Universität Darmstadt, Institute of Materials Science, Surface Science Division, Petersenstrasse 32, D-64287 Darmstadt, Germany*
[3]*SINTEF-Materials and Chemistry Syntesis and Properties, Forskningsveien 1, Pb. 124 Blindern, 0314 Oslo, Norway*
[4]*Department of Materials Science, School of Chemistry, Madurai Kamaraj University, Tamil Nadu, Madurai, India*
[5]*Department of Physics/Centre for Materials Science and Nanotechnology, University of Oslo, 0316 Oslo, Norway*

(Received 27 October 2012; accepted 20 December 2012; published online 17 January 2013)

The interface between indium tin oxide and p-type silicon is studied by *in situ* X-ray photoelectron spectroscopy (XPS). This is done by performing XPS without breaking vacuum after deposition of ultrathin layers in sequences. Elemental tin and indium are shown to be present at the interface, both after 2 and 10 s of deposition. In addition, the silicon oxide layer at the interface is shown to be composed of mainly silicon suboxides rather than silicon dioxide. © *2013 American Institute of Physics*. [http://dx.doi.org/10.1063/1.4774404]

Despite the growing number of available transparent conducting materials (TCMs), indium tin oxide (ITO) is still the most preferable TCM for a number of applications due to its excellent electrical and optical properties.[1] When ITO is deposited on a Si substrate a thin (1–3 nm) silicon oxide (SiO_x) layer is established, due to the thermodynamics of this formation.[2] The properties of this interfacial layer may influence the operation of a device, such as solar cells.[3] For instance, Goodnick *et al.* showed a thermal degradation of ITO/p-Si solar cells due to growth of additional interfacial SiO_x.[4]

X-ray photoelectron spectroscopy (XPS) is a suitable characterization method for the study of physical and chemical properties of the SiO_x layer and the ITO/Si interface. Chemical analysis of bonds between elements in an ITO/Si interface is previously carried out by the use of *ex situ* XPS of ultrathin ITO films on monocrystalline Si and XPS depth profiling of ITO on monocrystalline silicon and amorphous silicon.[5–7]

XPS is a characterization method which is sensitive to surface contamination. For instance, carbon impurities are previously proven to affect the work function value of ITO measured by XPS.[8] Thus, in order to avoid influence by any contamination, a cleaning procedure prior the spectroscopy is required. Cleaning the sample by ion bombardment will remove most of the impurity elements, though, some atoms will still remain at the surface. A drawback of ion bombardment is that it may induce side-effects such as chemical changes in the material, as described in Ref. 9, and references therein. One type of chemical change can be depletion of certain elements when the material is a compound. This can either be due to different sputtering yield or due to preferential sputtering caused by higher volatility of one element. In the case of a metal oxide, such depletion might induce a reduction in the oxidation state of the metal. Other chemical changes would be the effect of "knock on" (Ref. 9), which is an incorporation of elements further into the material during sputtering. Another side-effect of ion bombardment is the topological changes at the sample surface, also described in Ref. 9. For both sample cleaning and depth profiling XPS, the possibility of chemical changes must be taken into consideration.

A method which can overcome the influence of contamination and cleaning procedures is *in situ* XPS. Without breaking vacuum after material deposition, it is possible to carry out XPS studies of ultrathin layers step by step during growth of a thicker film, not influenced by contamination. This paper presents an *in situ* XPS study of ITO deposited by rf magnetron sputtering onto a monocrystalline silicon substrate at room temperature. It investigates the initial stages of the growth of the ITO film on a Si wafer, which includes the formation of a SiO_x interfacial layer and the presence of metallic indium and tin at the interface.

The ITO was deposited onto a polished p-type Czochralski Si substrate of size 2×2 cm. The orientation of the silicon crystal was $\langle 100 \rangle$ and the resistivity 1–3 Ωcm. Prior deposition, the substrate was etched in hydrofluoric acid (HF) (5 vol. %) in order to remove any native SiO_x. The substrate was rinsed in deionized (DI) water (18 MΩcm) and blown dry with nitrogen. Subsequent to this treatment, the substrate was mounted to the sample holder and transferred quickly, in nitrogen atmosphere, to the load lock of DAISY-MAT (DArmstadt Integrated SYstem for MATerial research). This system is described in Ref. 10. XPS was carried out on the silicon substrate prior to the depositions. As both the deposition chamber and the X-ray spectrometer are connected to DAISY-MAT, the sample was transferred back and forth from deposition to spectroscopy, without breaking the vacuum. The ITO layers were deposited at room

[a]Author to whom correspondence should be addressed. Electronic mail: margrethe.rein@gmail.com.

 © 2013 American Institute of Physics

temperature in four steps of 2, 8, 30, and 900 s, giving a total deposition time of 940 s. The substrate to target distance was 10 cm, the working power was 25 W (power density of $\sim$1.2 W/cm^2) and the working pressure was 5×10^{-3} mbar. The flow of argon during sputtering was 6 sccm and the target composition was 90 wt. % In_2O_3 and 10 wt. % SnO_2.

XPS was carried out using a Physical Electronics PHI 5700. Monochromatic Al Kα radiation ($h\nu = 1486.6$ eV) was employed as excitation for XPS. XP spectra of In 3 d, Sn 3d, O 1s, and Si 2p were recorded with a take-off angle of 45°. The XPS results were peak fitted using the fitting program CasaXPS. The background type was Shirley and the fitting components were Guassian/Lorenzian (30%/70%) product formulas. Some of the components were also modified by the exponential blend, due to the metallic state of elements.

Cross-sectional transmission electron microscopy (TEM) samples were prepared by ionmilling using a Gatan precision ion polishing system with 5 kV gun voltage. The samples were analyzed by high-resolution TEM (HRTEM) and energy filtered TEM (EFTEM) in a 200 keV JEOL 2010 F microscope with a Gatan imaging filter and detector. The spherical (Cs) and chromatic aberration (Cc) coefficients of the objective lens were 0.5 and 1.1 mm, respectively. The point to point resolution was 0.194 nm at Scherzer focus (42 nm).

Secondary ion mass spectroscopy (SIMS) measurements were carried out by the use of a CAMECA ims 7f instrument. The elements were ionized in negative mode with a 15 keV primary ion beam of Cs+, and the sputtering time was 42 480 s. The depth of the sputtered craters was measured with a Dektak 8 surface stylus profilometer.

Figure 1 shows the XPS spectra of In $3d_{5/2}$, Sn $3d_{5/2}$, O 1s, and Si 2p carried out prior and subsequent to the depositions. The In $3d_{5/2}$, Sn $3d_{5/2}$, and O 1s spectra are fitted with two or three components, while the Si 2p spectra from substrate and after 2, 10, and 40 s deposition are fitted with two, five, six, and one $Si_{3/2}$ and $Si_{1/2}$ peaks, respectively. No In or Sn peaks are observed prior deposition and no Si peaks after the last deposition. The thicknesses are estimated from TEM images and calculations based on the integrated area of the Si peaks in the XPS spectra.[11]

The predominant peaks in the In $3d_{5/2}$ and Sn $3d_{5/2}$ spectra after the first deposition for 2 s are attributed to elemental In and Sn, following a similar analysis procedure as in our previous work.[12] Pure In is also found after 10 s, while pure Sn is present both after 10 and 940 s. A segregation of tin to the film surface is previously reported by others.[13] The mentioned analysis is performed for the predominant In_{II} and Sn_{II} peaks after 10, 40, and 940 s as well, and these peaks are assigned to In and Sn in crystalline ITO.

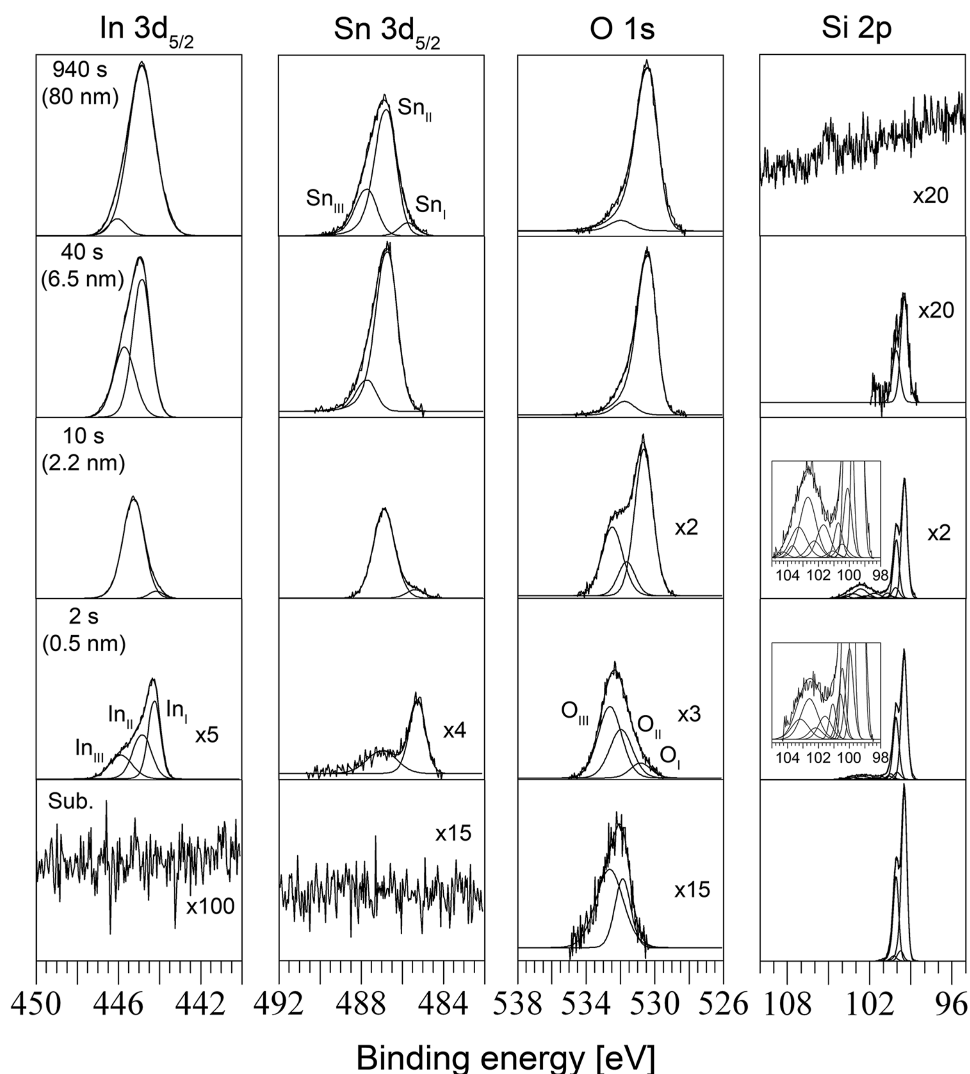

FIG. 1. The XPS spectra and peak fitting of the In $3d_{5/2}$, Sn $3d_{5/2}$, O 1s, and Si 2p peaks. The Si 2p spectra include SiO_x insets. The intensities of some spectra are enhanced with the indicated factors.

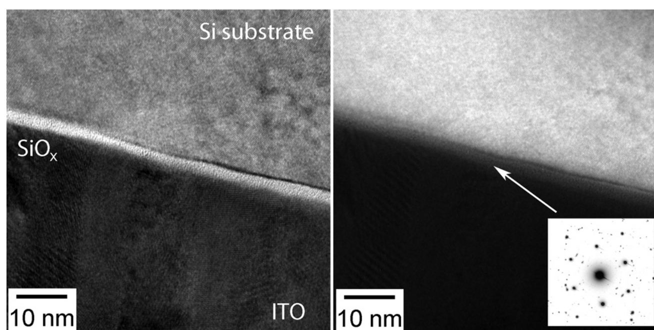

FIG. 2. Energy filtered TEM images using the plasmon peak of (a) SiO_2 at 23 eV, and (b) for Si at 16 eV.

In the previous work, we argued that In components at 444.9 eV and 446.0 eV (energy separation of 1.1 eV) could be attributed to crystalline and amorphous ITO, respectively.[12] By further examination, applying the electroneutrality principle, the presence of amorphous ITO has been excluded.[13] We can confirm this conclusion by analysis of TEM images (Fig. 2) showing no diffuse circles in the diffraction pattern.

The origin of the minor peaks In_{III} (at 445.9, 445.7, and 446.0 eV after 2, 40, and 940 s, respectively) and Sn_{III} (487.7 and 487.5 eV after 40 and 940 s, respectively) could be related to hydrogen, as hydrogen was detected by SIMS in both bulk and interfacial ITO (Fig. 3). The position of the In_{III} component coincides with the $In(OH)_3$ state (445.8 eV) in Ref. 14. Similarly, the high binding energy peak Sn_{III} could be assigned to bonds between hydrogen and Sn. Another explanation could be plasmon excitation. This is previously discussed by Christou *et al.*[15] and Gassenbauer *et al.*[16]

The two O 1s components found at the Si wafer surface (531.9 and 532.6 eV) are most likely due to water molecules and contamination adsorbed at the substrate surface, originated from the DI water rinsing or exposure to air. The values coincide with the binding energies for hydroxides, contamination, and oxygen due to air exposure (531.7 ± 0.2 and 532.7 ± 0.2 eV) reported by Plá *et al.*[17] Hydroxides are plausible as the substrate was cleaned in HF and rinsed in DI water. OH groups at Si(100) wafers after HF etch and DI water rinsing are previously detected using high resolution electron energy loss spectroscopy (HREELS).[18] Contamination due to air exposure is also plausible as traces of carbon were detected at the substrate surface and after 2 s deposition (not illustrated).

After 2 s of deposition, the predominant O 1s peak is at 532.6 eV (O_{III}). The intensity of this peak increases slightly after the next deposition (not illustrated in the figure) and disappears after further deposition. Hence, this binding energy is more likely due to other chemical states than found at the substrate surface. An obvious explanation of the origin would be compounds of oxygen and silicon as SiO_x is observed as a shoulder after 2 and 10 s in the Si 2p spectra (discussed below). A binding energy of 532.6 eV is reported by Wagner *et al.* of thermally oxidized silicon wafer.[19] The interfacial SiO_x layer is also observed by TEM and SIMS in Figs. 2 and 3, respectively.

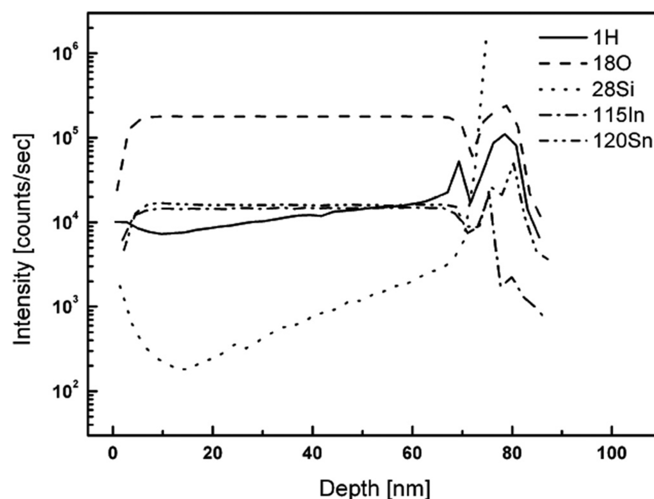

FIG. 3. SIMS of the ITO/Si interface and SiO_x interfacial layer.

The analysis of the O_I and O_{II} components found after deposition is similar to our previous work.[12] Both peaks are attributed to crystalline ITO, the O_{II} component related to O^{2-} ions at oxygen deficient sites.

The binding energy, full width at half maximum (FWHM), and chemical shift of the Si 2p and SiO_x peaks were fitted as shown in our previous work.[20] In addition to the Si 2p peaks corresponding to the $2p_{1/2}$ and $2p_{3/2}$ spin states, two small components with binding energy in the range 99.8 - 100.6 eV are found. These small components are attributed to silicon bonded to hydrogen, according to Thøgersen *et al.*[20] In that work, a peak with binding energy at 99.7 eV was attributed to Si_3SiH and is close to our value (99.8 eV). The two small components at 100.1 and 100.6 eV after 10 s can be attributed to Si_2SiH_2, which has a binding energy 0.57 eV higher than elemental Si.[21]

The SiO_x shoulder with a peak position at 102.6 eV is fitted by three and four components after 2 and 10 s deposition, respectively. The components in the decomposed SiO_x peak correspond to the Si_2O, SiO, Si_2O_3 (suboxides) and SiO_2 states. No SiO_2 is found after 2 s deposition and the predominant peaks correspond to the Si_2O and Si_2O_3 suboxide states. After 10 s deposition, the Si_2O_3 peaks are predominant and small peaks corresponding to the SiO_2 state are present. These results show that SiO_2 is not the dominating oxide in the SiO_x interfacial layer between ITO and Si.

From the literature, it is known that oxidation of suboxides requires heat at a certain level. He *et al.* found that suboxides oxidize into SiO_2 when annealing at high temperatures (>1000 K).[22] Zhang *et al.* reported changes in concentration of the different suboxides due to increased annealing temperature, though low annealing temperature ($<400\,°C$) did not change the concentration of Si_2O and Si_2O_3 states.[23] According to this information, we assume that the presence of SiO_2 in the SiO_x layer is significantly low throughout the layer as our sample did not undergo heat treatment.

The presence of suboxides may introduce another band gap than SiO_2 in the SiO_x layer. A narrower band gap for suboxides in a SiO_2/n-type Si(111) interface region is calculated by Yamashita *et al.*[24] They have shown that the main oxides in a thin interface region between a Si substrate and a SiO_2 film are Si_2O and Si_2O_3 and that the band gap increases

as the oxidation state increases ($E_g(Si_2O) < E_g(Si_2O_3) < E_g(SiO_2)$). A different band gap alignment of the ITO/Si interface than in the case of SiO_2 as the main silicon oxide and the presence of metallic In and Sn at the interface may play a significant role in the carrier transport mechanism in the ITO/Si junction. The prominent presence of suboxides at the ITO/Si interface and the likely effect on the tunneling probability through the SiO_x layer has previously been put forward by Kobayashi *et al.*[25]

In conclusion, this *in situ* XPS study qualitatively confirms previous *ex situ* XPS results. We have shown that both elemental In and Sn are present at the ITO/Si interface. Our study also reveals that suboxides are predominant in the interfacial SiO_x layer. This may have an impact on the carrier transport properties at the ITO/Si interface.

The authors would like to thank Lasse Vines for performing the SIMS characterization. The work was funded by REC Solar, the Research Council in Norway, through the Nanomat program, and the XPS work in Darmstadt has been supported by the Deutsche Forschungsgemeinschaft (DFG) within the collaborative research center SFB 595.

[1] S. Ray, R. Banerjee, N. Basu, A. Batabyal, and A. Barua, J. Appl. Phys. **54**, 3497 (1983).
[2] C. Ow-Yang, Y. Shigesato, and D. Paine, J. Appl. Phys. **88**, 3717 (2000).
[3] J. Shewchun, J. Dubow, C. Wilmsen, R. Singh, D. Burk, and J. Wager, J. Appl. Phys. **50**, 2832 (1979).
[4] S. Goodnick, J. Wager, and C. Wilmsen, J. Appl. Phys. **51**, 527 (1980).
[5] S. Diplas, O. M. Lovvik, H. Nordmark, D. M. Kepaptsoglou, J. M. Graff, C. Ladam, F. Tyholdt, J. C. Walmsley, A. E. Gunnaes, R. Fagerberg, and A. Ulyashin, Surf. Interface Anal. **42**, 874 (2010).
[6] A. Montesdeoca-Santana, E. Jimenez-Rodriguez, N. Marrero, B. Gonzalez-Diaz, D. Borchert, and R. Guerrero-Lemus, Nucl. Instrum. Methods Phys. Res. B **268**, 374 (2010).
[7] S. Sheng, H. Hao, H. Diao, X. Zeng, Y. Xu, X. Liao, and T. L. Monchesky, Appl. Surf. Sci. **253**, 1677 (2006).
[8] K. Sugiyama, H. Ishii, Y. Ouchi, and K. Seki, J. Appl. Phys. **87**, 295 (2000).
[9] J. C. Riviere, *Practical Surface Analysis by Auger and X-ray Photoelectron Spectroscopy*, edited by D. Briggs and M. P. Seah (Wiley, Chichester, 1983), pp. 17–85.
[10] D. Ensling, A. Thissen, Y. Gassenbauer, A. Klein, and W. Jaegermann, Adv. Eng. Mater. **7**, 945 (2005).
[11] M. P. Seah, *Practical Surface Analysis by Auger and X-ray Photoelectron Spectroscopy*, edited by D. Briggs and M. P. Seah (Wiley, Chichester, 1983), pp. 181–216.
[12] A. Thøgersen, M. Rein, E. Monakhov, J. Mayandi, and S. Diplas, J. Appl. Phys. **109**, 113532 (2011).
[13] J. Kim, P. Ho, D. Thomas, R. Friend, F. Cacialli, G. Bao, and S. Li, Chem. Phys. Lett. **315**, 307 (1999).
[14] C. D. Wagner, *Practical Surface Analysis by Auger and X-ray Photoelectron Spectroscopy*, edited by D. Briggs and M. P. Seah (Wiley, Chichester, 1983), pp. 477–509.
[15] V. Christou, M. Etchells, O. Renault, P. J. Dobson, O. V. Salata, G. Beamson, and R. G. Egdell, J. Appl. Phys. **88**, 5180 (2000).
[16] Y. Gassenbauer, R. Schafranek, A. Klein, S. Zafeiratos, M. Havecker, A. Knop-Gericke, and R. Schlogl, Phys. Rev. B **73**, 245312 (2006).
[17] J. Pla, M. Tamasi, R. Rizzoli, M. Losurdo, E. Centurioni, C. Summonte, and F. Rubinelli, Thin Solid Films **425**, 185 (2003).
[18] D. Graf, M. Grundner, R. Schulz, and L. Muhlhoff, J. Appl. Phys. **68**, 5155 (1990).
[19] C. Wagner, D. Passoja, H. Hillery, T. Kinisky, H. Six, W. Jansen, and J. Taylor, J. Vac. Sci. Technol. **21**, 933 (1982).
[20] A. Thøgersen, J. H. Selj, and E. S. Marstein, J. Electrochem. Soc. **159**, D276 (2012).
[21] G. Cerofolini, C. Galati, and L. Renna, Surf. Interface Anal. **35**, 968 (2003).
[22] J. He, X. Xu, J. Corneille, and D. Goodman, Surf. Sci. **279**, 119 (1992).
[23] W. Zhang, S. Zhang, Y. Liu, and T. Chen, J. Cryst. Growth **311**, 1296 (2009).
[24] Y. Yamashita, S. Yamamoto, K. Mukai, J. Yoshinobu, Y. Harada, T. Tokushima, T. Takeuchi, Y. Takata, S. Shin, K. Akagi, and S. Tsuneyuki, Phys. Rev. B **73**, 045336 (2006).
[25] H. Kobayashi, T. Ishida, Y. Nakato, and H. Tsubomura, J. Appl. Phys. **69**, 1736 (1991).

This article may be downloaded for personal use only. Any other use requires prior permission of the author and AIP Publishing. This article appeared in (Appl. Phys. Lett. 102, 021606 (2013)) and may be found at (https://doi.org/10.1063/1.4774404).

Available under only the rights of use according to UrhG.